Chapter 6

Graphene Aerogel-Directed Fabrication of Phase Change Composites

Guangyong Li, Xiaohua Zhang and Xuetong Zhang

Additional information is available at the end of the chapter

http://dx.doi.org/10.5772/intechopen.74616

Abstract

Although phase change materials have been extensively used for thermal energy storage, various shortcomings such as low thermal conductivity, leakage during work, and shortage of multiple driving ways greatly hinder their practical applications. Among the new materials that can overcome these problems, graphene aerogel has attracted special interest owing to its 3D conductive network and extraordinary capillary force. In this chapter, we review recent progress of graphene-aerogel-based phase change composites (PCCs) and provide a brief introduction on the following topics: 1) why graphene aerogels can be used for PCCs, 2) the sol-gel transition synthesis of graphene aerogels, 3) the fabrication of graphene-aerogel-based PCCs, and 4) their applications in thermal energy storage, electric-thermal conversion and storage, solar-thermal conversion and storage, and thermal buffer. Finally, we also discuss the limitation and future development of these graphene-based materials.

Keywords: phase change materials, aerogel, graphene, sol-gel, thermal energy

1. Introduction

Thermal energy storage technologies have played a broad and critical role in sustainable utilization of energy in heating and cooling apparatus, including vehicles and buildings, smart textiles with thermal comfort, electrochemical and electronic devices [1–3]. Phase change materials (PCMs) have been widely used in thermal energy storage technologies because they can absorb or release a great amount of energy as latent heat during the solid-solid or solid-liquid phase transitions over a narrow temperature range. In general, PCMs can be classified into organic (e.g., paraffin, fatty acids, and polyethylene oxide) and inorganic types (inorganic salts and their hydrates). The organic PCMs have attracted great attention in phase change

system as they exhibit high phase change enthalpy, wide melting temperature for convenient use, chemical stability and abundance in natural resources, besides the common properties of the inorganic ones. However, their practical applications are still hindered by various shortcomings of PCMs [4], such as the low thermal conductivity, leakage during melting process, and weak responsiveness to optical or electrical stimuli.

To resolve these disadvantages, scientists have tried to embed various PCMs into a lot of matrices, such as microcapsules and 3D porous materials (aerogel, foam, and sponge) with interconnected network [5–10]. The matrices can give the PCMs improved thermal conductivity, shape stability during melting process, and high absorption of sunlight or sufficient electrical conductivity for multiple driving ways. In principle, the ideal matrix should possess excellent thermal conductivity to improve the power capacity, extensive capillary force and high mechanical property to avoid leakage during working, lightweight framework to maintain high latent heat, and dark color and high electrical conductivity to store thermal energy via multi-driven ways (sunlight absorbing or Joule heating).

Graphene, a novel nanomaterial with two-dimensional (2D) planar crystal consisting of a single carbon atom layer, has many extraordinary properties including superior flexibility, strong mechanical strength, and excellent electrical and thermal conductivities [11]. However, graphene sheets usually tend to irreversibly aggregate or even re-stack back to graphite due to their intrinsic 2D conjugated structure, making it difficult to efficiently exploit the inherent properties of graphene [12]. There are several ways to resolve such problem by designing porous assemblies of graphene with a 3D interconnected network, namely, assembling into aerogel microspheres by a micro-droplet technology, into aerogel fiber with the help of spinning technology, and even into aerogel film and monolith. These different forms of graphene aerogel have the following common characters: low mass density, high porosity, robust mechanical performance, blackbody-like absorptive performance, electrically and thermally conducting, and extraordinary capillarity [12–14]. Therefore, multifunctional phase change composites (PCCs) can be developed based on these graphene aerogels, and are expected to exhibit superior performances including excellent conductivity, high latent heat, multiple driving ways (thermal, electrical, and optical), and no leakage for melt PCMs.

This chapter reviews recent and rapid progress on graphene-aerogel-based PCCs and discusses their future development. First, the fabrication of graphene aerogels based on sol-gel transition is described in Section 2. Then, Section 3 discusses in detail the synthesis of graphene-aerogel-based PCCs including microspheres, fiber, film, and monolith. Finally, the typical applications of PCCs are introduced in Section 4. This chapter may inspire many new explorations surrounding the PCM-based thermal energy storage.

2. Fabrication of graphene aerogel

Graphene aerogels can be prepared via both solution assembly and chemical vapor deposition (CVD) growth. The solution assembly technology is based on a sol-gel reduction process of graphene oxide (GO) solution and a subsequent specific drying [12, 14]. GO sheets are rich in

oxygen-containing functional groups that allow excellent dispersibility in water and polar organic solvent, promising the possibility to operate graphene sheets into aerogels. The CVD growth technology is usually performed on specific template (e.g., Ni foam or SiO_2 aerogel) during high temperature atmosphere that contains carbon source (e.g., CH_4 and ethanol), and the aerogel is obtained after removing the template [15, 16].

The solution assembly has become the most popular method to prepare graphene aerogels due to its cost-effective progress, high yield from cheap graphite, amenability to operation, and efficient utilization of the inherent properties of graphene [12]. The solution fabrication mainly involves the synthesis of graphene hydrogel, the aerogel precursor, and the subsequent drying process.

2.1. Synthesis of graphene hydrogel

The graphene hydrogel can be synthesized via a sol-gel transition of GO solution, together with a reduction process. After the reduction, the oxygen-containing functional groups on GO sheets can be removed, resulting in the recovery of strong π-π interaction and a transition from hydrophilicity to hydrophobicity [12]. It can also promote the gelation process to form a uniform graphene hydrogel, based on the partial overlapping and π-π stacking between the reduced GO (rGO) sheets [12]. Such sol-gel transition can be realized via a variety of reduced routes, such as chemical reduction [17], hydrothermal reduction [18], and electrochemical reduction [19].

Chemical reduction is a versatile and mild method, and can be performed in acidic or alkaline media by using different reducing agents, such as L-ascorbic acid (L-AA), HI, $NaHSO_3$, NaI/oxalic acid, dopamine, ethane diamine, and even metals (Zn) [14]. Notably, the agents used here should be mild and green, and can promote the formation of uniform graphene hydrogel without generating any gas. For example, by introducing L-AA into GO solution, mixing them uniformly, and then heating the mixture for a period of time without stirring, a uniform graphene hydrogel was obtained (**Figure 1a-b**) [17]. To understand the sol-gel transition, various factors like GO concentration, GO/L-AA mass ratio, temperature, time, and pH of the sol-gel reaction were investigated systematically [20]. For the GO/L-AA mixed solution, the GO concentration and L-AA/GO mass ratio are two key factors; the optimal GO concentration was found to be 1.0–6.0 mg/mL and the mass ratio could be in a very wide range 1:2–832:1. When the amount of GO was too small (<1.0 mg/mL) or L-AA was insufficient (L-AA/GO <1:2), it was difficult to induce the partial stacking and overlapping; on the contrary (GO >6 mg/mL or L-AA/GO >832:1), the uniform dispersion of GO or L-AA became difficult. Other parameters like a pH value of 7.0-3.0, a high temperature of 25–80°C, and a long aging time were also found to benefit the gelation rate and the hydrogel quality. Besides L-AA, other reducing agents have also been investigated. By using a similar sol-gel treatment, ethane diamine was dissolved in a GO solution to reduce the GO during the formation of graphene hydrogel, after being aged in 95°C for 6 h [21]. Such hydrogel was electrically conducting and mechanically robust, and exhibited a uniform gel network, being able to serve as an ideal precursor for aerogel.

However, under a low GO concentration, such as the aforementioned optimal 1.0–6.0 mg/mL, the obtained graphene aerogel usually exhibited a disordered porous network. For a better performance, is it possible to assemble GO sheets to an anisotropic graphene hydrogel with a

Figure 1. Digital photos of the aqueous suspension of graphene oxide (a), the graphene hydrogel in a vial (b), the graphene aerogels obtained by supercritical CO_2 drying and freeze-drying (c), and a graphene aerogel supporting a counterpoise (d) [17].

certain alignment or orientation of the pore or graphene sheets? As a successful demonstration, under a high-speed centrifugation, a highly concentrated GO dispersion exhibited a novel fluid crystal phase, namely, a GO liquid crystal (GO-LC). The GO sheets tended to orient parallel with each other, resulting in the ordered arrangement of GO sheets [22, 23]. However, the high viscosity of GO-LC brought new problems toward the uniform sol-gel transition, making the application of the conventional reduction routes no longer suitable for the preparation of graphene hydrogel.

Very recently, a novel sol-gel strategy was proposed to synthesize the anisotropic graphene hydrogel, by an in situ gelation of GO-LC using the gaseous hydrogen chloride (HCl (g)), and a subsequent chemical reduction as well (**Figure 2**) [24]. When a GO-LC is placed in HCl atmosphere, the HCl molecule can dissolve and diffuse slowly into the GO-LC, together with an immediate ionization, which promised the "in situ freezing" of dynamic hydrogen-bonding network and resulted in the generation of GO-LC hydrogel (**Figure 2**). Interestingly, the HCl treatment can also induce a typical colorful texture between crossed polarizers, due to the directional arrangement of GO sheets. Then, the GO-LC hydrogel can be immersed into HI (aq) to obtain an anisotropic graphene hydrogel with different macro-sizes and shapes. As no stirring and mixing operations are involved, the original arrangement of GO sheets can be well maintained in the final graphene hydrogel.

Importantly, the shape of graphene hydrogel can simply be controlled by changing the reactor or introducing a certain confinement effect. From the former way, graphene hydrogels with various shapes including cylinder, sphere, and rectangular solid have been reported. For the

http://dx.doi.org/10.5772/intechopen.74616

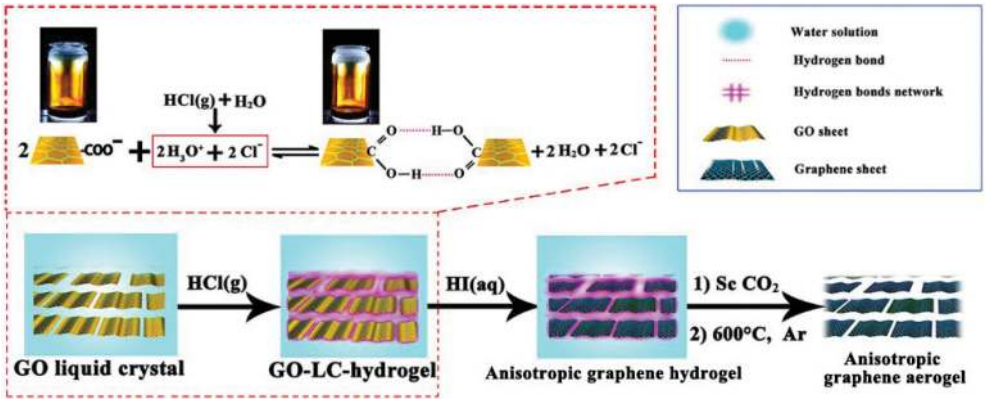

Figure 2. Schematic description of the synthesis of anisotropic graphene aerogels, derived from liquid crystals under the assistance of the solid hydrogen-bonded network, based on a vapor diffusion and sol-gel process [24].

latter, the micro-droplet, filming, and spinning techniques have been used to obtain the graphene hydrogel microsphere, film, and fibers.

2.2. Drying process

The obtained graphene hydrogel can be dried via some specific drying treatment to form a graphene aerogel. During the normal drying method, the graphene hydrogel undergoes a direct liquid-gas transition, where the remarkable change in capillary force causes the shrink and collapse of the porous network [25]. Therefore, in order to maintain the porous network, supercritical fluid drying or freeze-drying is suggested to replace the liquid solvent of graphene hydrogel with air, rather than by the direct liquid-gas transition [17, 25].

The supercritical fluid drying is realized in a supercritical state where the temperature and pressure are beyond the critical point. Supercritical CO_2 (Sc CO_2) has become the most widely used method due to its low critical temperature (31.1°C), no risk of combustion and toxic gas, and a moderate critical pressure (7.38 MPa). By the Sc CO_2 drying, graphene hydrogel can be converted into graphene aerogel successfully [17, 24]: 1) the liquid component of the original graphene hydrogel is replaced by an organic solvent (ethanol, acetone, methanol, etc.); 2) the obtained organogel is placed in a pressure vessel and then soaked in a flowing Sc CO_2 for a period time, until all the solvent in the porous network was replaced by Sc CO_2; and 3) a graphene aerogel is finally obtained after recovering the pressure vessel to ambient pressure.

For example, as shown in **Figure 1c**, a graphene aerogel with Sc CO_2 drying was obtained, which exhibited a certain darkness, high porosity, high specific surface area (512 m^2/g), large pore volume (2.48 cm^3/g), high electrical conductivity (~10^2 S/m), and high mechanical property; it could support at least 14,000 times its own weight (**Figure 1d**) [17].

The freeze-drying mainly involves the freezing and sublimate processes, and this drying can induce a solid-gas transition [25]. To prepare a graphene aerogel, a graphene hydrogel that contains plenty of water is first frozen at a low temperature (liquid N_2 or freezer), and then the

ice inside the pore starts to sublimate directly under vacuum, with the pore being filled by air [17, 26–28]. During the freeze-drying process, the growth of ice crystal usually causes reconstruction of the original network of hydrogel, together with an aggregation of the mesopores into a macropore. Then the resulting graphene aerogel usually shows a poor mechanical strength, high brittleness, low specific surface area, and little mesopore volume. As shown in **Figure 1c**, the graphene aerogel by freeze-drying showed a metal luster, but it could only support 3300 times its own weight [17]. Based on a N_2 adsorption/desorption test, the pore volume was 0.04 cm^3/g in the size range of 1.5–55 nm, which was much lower than that of the graphene aerogel by Sc CO_2 drying (2.48 cm^3/g), corresponding to the disappearance of mesopores.

3. The fabrication of graphene-aerogel-based PCCs

According to the different macroscopic architectures of graphene aerogels, the graphene-aerogel-based PCCs can be developed in forms of 0D microspheres, 1D fibers, 2D films, and 3D monoliths. The two widely used strategies for the fabrication of aerogel-based PCCs (e.g., carbon aerogel, carbon nanotube sponge, carbon nanotube array, graphene aerogel, and other aerogel matrices) are the melted filling and solvent-assisted filling [7–9, 24].

Above the melting point, the conventional PCMs will become liquid state. The melted PCMs can be infiltrated directly into the porous network of aerogel owing to aerogel's extraordinary capillary force, similar to the simple process of "sponge absorbing water". Thus, graphene aerogel could direct the fabrication of PCCs [24, 29]: immerse a graphene aerogel into a melted PCM, allow the pore space of aerogel be filled by the PCM, promise the melted PCM to be cooled inside the aerogel network, and then by removing the residue paraffin on the surface of composite, the relevant graphene aerogel-directed PCC could be obtained.

The solvent-assisted filling strategy can be performed by introducing a PCM solution into the internal space of aerogel. This method could avoid the limitation of temperature and high viscosity of the melted PCM [7]. First, a graphene aerogel is immersed into a PCM solution such as polyethylene glycol (PEG)/water, wax/CH_2Cl_2, stearic acid/C_2H_5OH. Then the PCM solution will flow into the porous network of aerogel, and then stay in the pores or get absorbed on the walls. After removing the solvent via natural volatilization, a PCC can be obtained. Notice that the densification and solidification effects from the solvent evaporation process may bring many fascinating properties.

Both the melted filling and solvent-assisted filling are based on the similar driving force—the capillary force of aerogel. There are also slight differences between these two methods, and they have their own scope of application. In the following sections, more detailed introduction is provided according to the shapes of microspheres, fibers, films, and monoliths.

3.1. 0D composite microsphere

To prepare graphene-aerogel-based PCC microspheres, the mono-dispersed graphene aerogel microspheres (GAMs) with 3D interconnected porous network should be produced first.

Unfortunately, the traditional strategies, including injection prilling, emulsion polymerization, and spray granulation, are not suitable for the fabrication of mono-dispersed GAMs [30–32], because the gelation should be realized in microdroplets and a long aging process is necessary.

Herein, based on the original sol-gel principle, a novel and programmable strategy has been developed, namely, an ink jetting-liquid marbling-supercritical fluid drying coupling technique, to produce mono-dispersed GAMs (**Figure 3a**) [33]. Typically, the valve ink jetting was used to synthesis the GO/L-AA droplets because it had a much wider size window and could precisely control the droplet size. The obtained mixed microdroplets were then dropped into a specific container fully filled with hydrophobic nanoparticles to form liquid marble. The liquid marbling technology could keep individual droplets separated from each other and maintain spherical structure without amalgamation. Once the injection was completed, the container

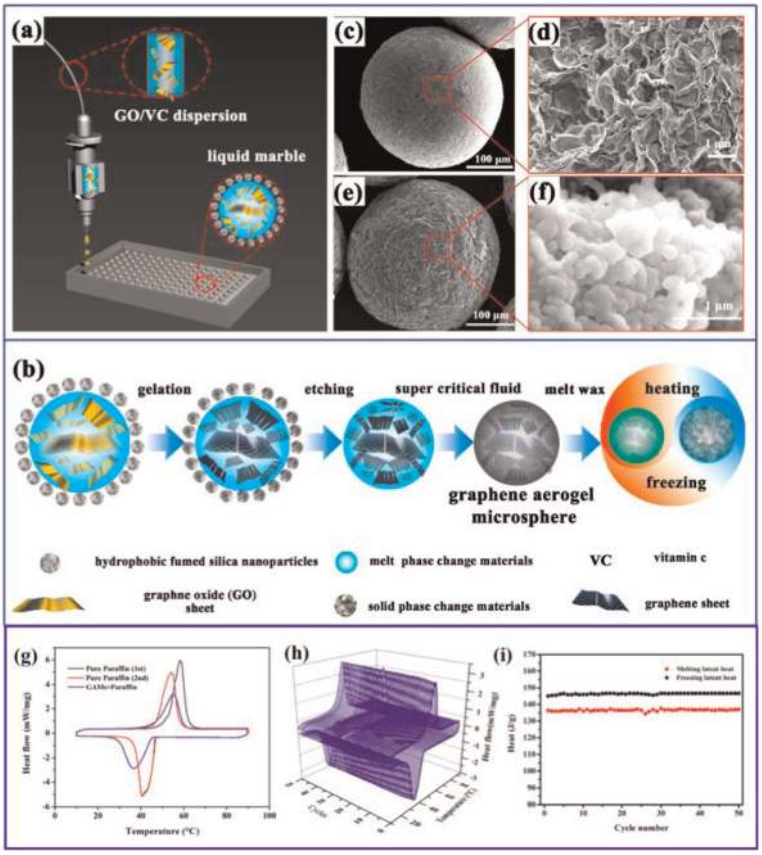

Figure 3. Schematic and results of the "ink jetting−liquid marbling−supercritical drying" coupling approach to make graphene aerogel microspheres and phase change microspheres [33]. (a) the ink jetting of sol droplet precursor. (b) the preparation of GAMs and phase change microspheres. (c-f) SEM images of a GAM (c,d) and a PCC microsphere (e,f). (g) Cyclic DSC curves of the paraffin and GAM-based PCC microspheres. (h,i) DSC curves and the corresponding latent heats of the PCC microspheres tested in 50 cycles.

was sealed and a sol-gel transition was triggered. Thus, GAMs with 3D interconnected graphene porous network could be fabricated by supercritical drying (**Figure 3c-d**). By adjusting the size of microdroplets, the size of graphene hydrogel microspheres could be efficiently controlled. Based on a statistical analysis on the size distribution of graphene hydrogel microspheres, the variation coefficients were 6.4, 4.9, and 5.6%, for the graphene hydrogel microspheres with an average size of 170, 200, and 230 μm, respectively, indicating that the ink jetting and liquid marbling techniques showed a superior advantage to produce uniform-sized GAMs.

By the melted filling, the PCM could be introduced into the inner pore spaces of GAMs, and the relevant graphene aerogel-directed PCC microspheres were obtained [33]. These microspheres exhibited good sphericity, and owing to the continuous conducting network of graphene aerogel and phase change ability of paraffin, they also exhibited a high latent heat (136 J/g, **Figure 3g**), excellent cyclic stability (**Figure 3h** and **i**). Furthermore, the microspheres (diameter ~700 μm) could respond to a weak heat (as low as 0.027 J) very sensitively, together with fascinating electrical properties, remarkable mutation of electrical resistance; the resistance was about 1370 Ω for the solid and 4850 Ω after being melted.

3.2. 1D composite fiber

Phase change fiber, also named as smart thermoregulating fiber, can buffer the environmental temperature variation by absorbing/releasing thermal energy. So far, the preparation of PCC fiber is mainly based on composite spinning, including wet-spinning, melt-spinning, and electrospinning [34–36]. For example, pure PCM or microencapsulated PCM can be mixed into polymer solution or its melt, which can be later spun into fibers [37]. However, the obtained fibers did not show a high enthalpy and their repeatability was quite low. It is still of strong requirement to develop new-type PCC fibers, via a novel and facile approach.

Graphene aerogel fiber (GAF) consisting of aligned graphene porous network can provide a successful template toward such development. The GAF can be prepared by both freeze-dry spinning and wet-spinning based on GO-LC. Such aerogel fibers usually contain interconnected porous network of aligned graphene sheets, and thus also exhibit high porosity, large specific surface area, excellent conductivity, and high flexibility. For example, a GAF with a unique "porous core-dense shell" structure was produced by a freeze-dry spinning, a combination of spinning and ice-templating strategy [38]. The obtained GAF showed a high electrical conductivity of 2.0×10^3 S/m, high mechanical strength (11.1 MPa), and large specific surface area (~884 m^2/g). At the same time, another GAF with aligned porous network was obtained by spinning GO-LC into specific coagulation bath which contained a reducing agent, such as HCl/L-AA (aq), HCl/HI (aq), acetone/HI (aq), $CaCl_2$/HI (aq), aniline hydrochloride/HI, followed by an aging process and specific drying. Such aerogel fiber exhibited a high mechanical strength (up to 18.1 MPa), high specific surface area (~548 m^2/g) and a large pore volume (~2.28 cm^3/g). In a different way, by injecting a GO/L-AA or GO/HI mixed solution into a micro-tube, after aging for a period of time under water bath and a following supercritical drying or freeze-drying, GAFs with excellent electrical conductivity and high flexibility property can be obtained [39].

Based on the obtained aerogel fiber, the aerogel-directed PCC fibers with variable phase change enthalpy and other thermal properties can be fabricated, by a solvent-assisted filling. By carefully adjusting the PCM materials and filling process (concentration, temperature, aging time, etc.), the mechanical, electrical, and thermal properties were tunable. For example, after introducing PEG-4000 (average molecular weight 4000), the obtained graphene/PEG PCC fiber exhibited a tunable phase change enthalpy of 28–116 J/g, depending on the PEG fraction, at a constant melting point of 54°C of the pure PEG-4000, see **Figure 4b**. The phase change enthalpy and melting point can also be efficiently adjusted in a wide temperature range by using different PCMs. For example, by using n-eicosane, the melting point could be just 36°C, and the enthalpy was as high as 186 J/g (**Figure 4c**).

3.3. 2D composite film

As compared to the 0D and 1D PCCs, a planar phase change film could provide a larger thermal exchange interface for thermal management in portable electronic devices. By combining the conventional filming technique [40–42], such as wet-spinning and blade-coating, with sol-gel transition and specific drying processes, graphene aerogel films with interconnected porous network can be produced.

Typically, GO-LC was spun via a wide spinning channel into a coagulation bath containing reducing agent (e.g., HCl/HI (aq), $CaCl_2$/HI (aq)) [41]. By such treatment, the fluid GO-LC would convert to a gel film, which was then being aged for 12 h. After a supercritical drying or

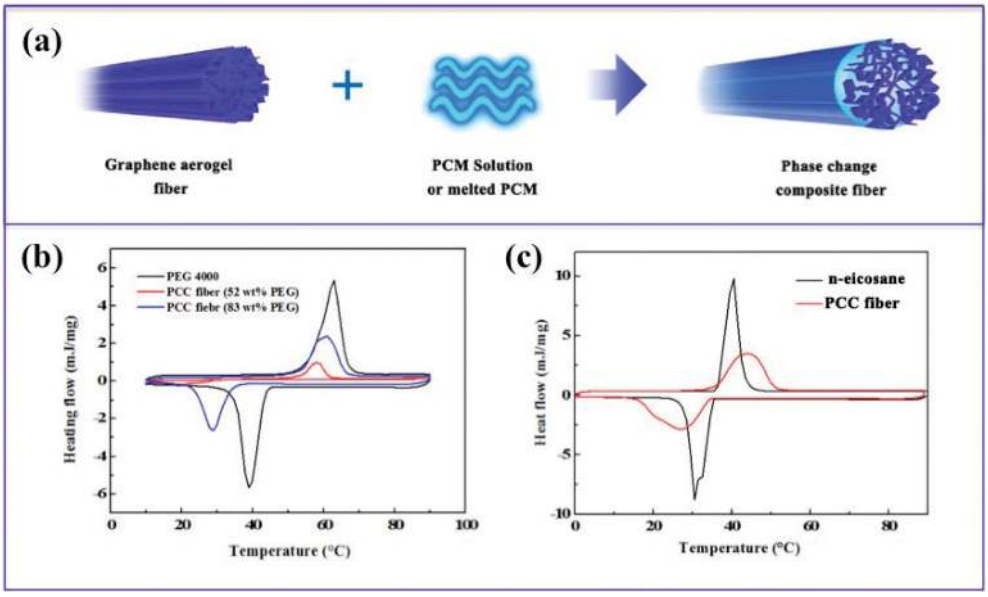

Figure 4. Aerogel-directed fabrication of graphene-aerogel-based PCC fiber. (a) Schematic description of the fabrication. (b,c) DSC curves of the PCC fibers, and for a comparison, the DSC result of PEG4000, and n-eicosane are plotted.

freeze-drying, a continuous graphene aerogel film was obtained. In another method, a high concentration GO dispersion or GO hydrogel was spread onto a glass substrate and a uniform GO hydrogel film could be obtained [42]. To reduce the GO, such hydrogel film was immersed into HI solution to obtain a flexible and free-standing graphene aerogel film by a supercritical drying process.

Based on the melted filling or solvent-assisted filling, the PCMs could be introduced for fabricating flexible and free-standing PCC films (**Figure 5**). For example, by immersing a graphene aerogel film into melted n-eicosane for about 3 h, a flexible composite film with a high latent heat (161 J/g) and low melting point (about 36°C) was obtained. As shown in **Figure 5b**, the PCC film exhibited a similar phase change behavior to pure n-eicosane.

3.4. 3D composite monolith

PCC monolith is the most widely used form for thermal energy storage due to their intrinsic bulk energy density. For a good heat transfer through a bulk PCC, the continuous and thermal conductive network is necessary. By considering its 3D porous network and high ability to conduct heat and current, graphene aerogel can serve as an important template to develop PCC monoliths.

The graphene-based PCC monoliths have been synthesized by melted filling. By immersing a bulk graphene aerogel into a melted PCM with the aid of vacuum, the inner pore spaces of aerogel can be fully filled by the PCM molecules. After a following cooling treatment, a PCC monolith can be obtained. For example, an anisotropic composite monolith was reported based on a composition of paraffin with a graphene aerogel with aligned pore structure, as shown in **Figure 6** [24]. Such PCC monolith contained a high paraffin loading up to 93.6 wt% with an enthalpy of 193.7 J/g. This special alignment of graphene network also induced a high anisotropy of the thermal conductivity, along the graphene sheet, the thermal conductivity could reach to 2.99 W/mK, about 15-fold higher than that of pure paraffin, higher than that of carbon nanotube array/n-eicosane composite; in other direction, the thermal conductivity exhibited a lower value of 1.2 W/mK.

A different method of hydrothermal reduction was also used to synthesize PCC monoliths [43]. To do so, a GO solution was mixed with a paraffin/cyclohexane solution, under a violent

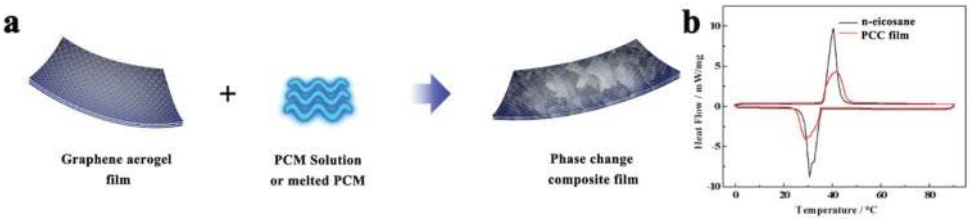

Figure 5. The preparation and thermal property of graphene-aerogel-based PCC film. (a) Schematic of preparation. (b) DSC curves of PCC film and n-eicosane.

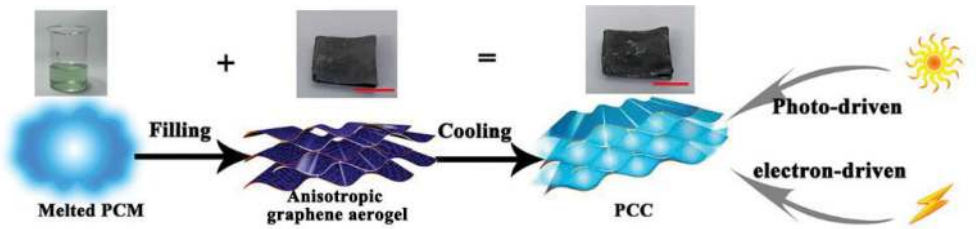

Figure 6. Illustration of the fabrication process in which the melting paraffin fills in the anisotropic graphene aerogel to make a composite that can be driven either electrically or optically for heat storage [24].

shaking to make the mixture (emulsion) homogeneous. Then, by a high temperature-induced reduction under a hydrothermal condition, and a following freeze-drying process, a PCC with encapsulated structure and continuous graphene network was obtained. By adjusting the concentration of the paraffin solution, a high PCM loading could be up to 97 wt%. Under such high loading, a good shape stability was still maintained as reflected by the zero PCM leakage, because the paraffin was encapsulated into the closed pore shell of graphene aerogel, to form micrometer-scaled droplets. Unfortunately, the thermal conductivity of such PCC monolith was just 0.274 W/mK, just comparable to that of the pure PCM (0.207 W/mK) [43].

4. Applications of graphene-aerogel-based PCCs

An intrinsic phase transition and high latent heat of PCMs, and their excellent physicochemical properties, would allow these graphene-aerogel-based PCCs to be applied in many fields with extraordinary performances.

4.1. Thermal energy storage

Among the various applications, thermal energy storage is the most fundamental application. It requires a superior thermal performance of PCM, including high thermal conductivity, high latent heat, excellent thermal cycling stability, and no leakage during work [24]. So far, graphene-aerogel-based PCCs have shown many advantages in thermal energy storage owing to the synergistic effect between graphene network and PCM.

Thermal conductivity is the most important property as it determines severely the power capacity of PCMs. Owing to the graphene network, the conductivity of graphene-aerogel-based PCCs were all much higher than that of pure PCMs. For example, based on a CVD-based graphene foam, the conductivity of the graphene/paraffin PCCs was up to 3.61 W/mK, 18 times higher than that of paraffin (0.2 W/mK) [3]. The similar enhancement was also observed for a rGO/octadecanoic acid PCC (from 0.18 W/mK for the pure octadecanoic acid to 2.6 W/mK) [44]. By using an anisotropic graphene aerogel, there was also an anisotropy in thermal conductivity (**Figure 7a**) [24]: the in-plane thermal conductivity was up to 2.99 W/mK,

while along the perpendicular direction it was just 1.2 W/mK (**Figure 7b**). Such anisotropy could provide a chance for rapidly storing heat along the parallel direction, and slowly releasing the heat along the other direction, making the heat usage more efficiently.

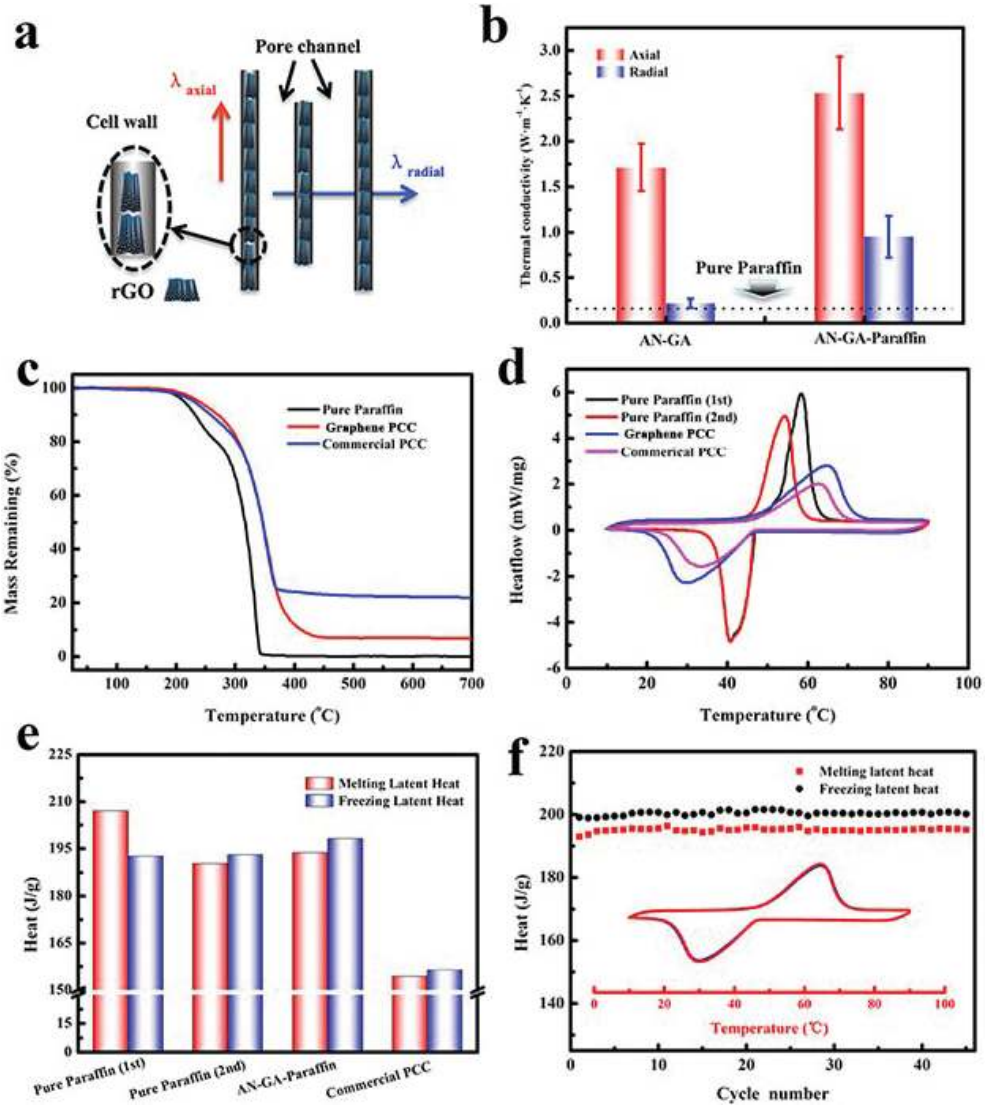

Figure 7. Thermal properties of an anisotropic graphene-based PCC monolith. (a) Schematic illustration of anisotropic heat transfer. (b) Thermal conductivities of the anisotropic graphene aerogel and the relevant PCC. (c,d) TGA and DSC curves of the pure paraffin, the commercial composite and the anisotropic graphene aerogel/paraffin PCC. (e) the measured latent heats obtained from (d). (f) Cyclic behaviors of the latent heat of the PCC during 45 melting-freezing cycles. The inset shows the 45th DSC curve which is fully identical to the first one in (d) [24].

Phase change enthalpy is another important characteristic, as it corresponds to the energy density. Although the introduction of graphene aerogel might affect the enthalpy of PCM slightly, the enthalpy of the overall PCC could be as high as the pure PCM. On the other hand, the presence of graphene could also benefit the crystallization of PCM, as a remedy to the enthalpy loss. Therefore, the full potential of PCM could still be realized in the PCC. For example, for a PCC monolith at a paraffin loading of 94 wt% (**Figure 7c**), the enthalpy was measured to be 193 J/g (**Figure 7d-e**), just ~6 wt% smaller than that of pristine paraffin (208 J/g). Nevertheless, such value was slightly higher than the secondary crystallization of pure paraffin (190.2 J/g) [24]. Furthermore, the porous network of graphene aerogel could promise the PCC to possess an excellent thermal stability between cyclic heating and cooling, as confirmed by the cyclic DSC curves (**Figure 7f**), and this excellent thermal stability also be found in other forms of PCC (0D, 1D, and 2D), as shown in **Figures 3–5** [26].

4.2. Electric-thermal conversion and storage

Electric-thermal conversion and storage based on PCM technique is important for effective utilization of power from off-peak electricity and renewable energy sources (e.g., wind and solar) [45]. As the basic property for electric-thermal conversion, high electrical conductivity of PCM is required. Unfortunately, the conventional PCMs are usually not an electrical conductor, and thus not available for electric-thermal conversion. For graphene-aerogel-based PCCs, the graphene network not only improves the thermal conductivity, but also exhibits many advantages in the electrical performances. As a result, when a current is passing thorough a PCC, the electric-thermal effect can be triggered by the graphene porous network, and the converted energy will be absorbed and stored by the PCM in the PCC [24].

Figure 8a shows the setup to evaluate the electro-thermal conversion and energy storage: a cylinder PCC monolith was connected into a DC circuit, and then the temperature evolution of PCC was recorded by a data collection system [24]. Under a constant voltage of 1.5 V, the PCC temperature increased rapidly during the first 45 s, and then reached a plateau until ~190 s, corresponding to the melting of paraffin (**Figure 8b**). After the full melting, the temperature started to increase again and much more rapidly. When the voltage was turned off, the

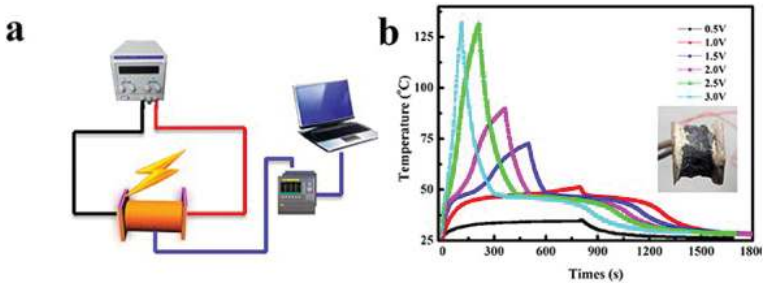

Figure 8. (a) Schematic illustration of the electro-driven phase change composite device circuit. (b) the temperature-time relationship of AN-GA-paraffin under different voltages [24].

temperature declined immediately to the freezing point (about 48°C) of paraffin, and another plateau was formed, corresponding to the solidification of paraffin. After the solidification stopped, the temperature would decrease again to room temperature. Via the temperature curves under different voltages, a critical voltage for a complete phase change was found to be about 1.0 V, which was a quiet low threshold compared to carbon aerogel (15 V) [8] and carbon nanotube sponges (1.5 V) [7].

4.3. Solar-thermal conversion and storage

Solar-thermal energy conversion and storage were essential for harvesting and utilizing of abundant solar energy. Both graphene aerogel and its directed PCC exhibited black appearance and high thermal conductivity, promising the application in solar energy.

To characterize the ability to convert solar energy [24], the graphene-aerogel-based PCC was placed under a solar simulator, by a tungsten-halogen lamp (**Figure 9a**). Without infiltrating any PCM into the graphene aerogel, the temperature of aerogel could increase up to 40–75°C under different light intensities, indicating that the graphene was a nice photo absorber (**Figure 9b**). For the graphene-aerogel-based PCC, due to the phase change, temperature plateaus (around 48°C) were observed during the solar-induced heating and cooling processes (**Figure 9c**), corresponding to an efficient energy storage. By dividing the stored thermal energy (from the product of enthalpy and PCC mass) by the irradiating energy overall received during the working time for the plateau, the conversion-storage efficient could reach to 77% (1.0 sun).

4.4. Thermal buffer

Graphene-aerogel-based PCC microspheres could serve as thermal buffer in electronic devices, as besides the ability to store the energy by Joule heating, they have also shown a fascinating electrical property.

To show such effect, a single graphene-based PCC microsphere was connected to a DC power by Cu wires (**Figure 10a**) [33]. Upon increasing the voltage, the current passing through the microsphere increased linearly until a critical point, where the Joule heating could have increased the temperature up to the melting temperature of PCM. Due to the PCM melting,

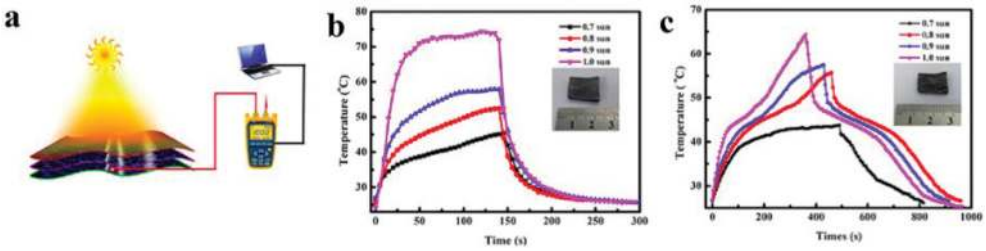

Figure 9. (a) Schematic of the characterization of solar-thermal conversion. (b,c) Temperature-time relationship under simulated sunlight (AM 1.5) at intensities of 0.7 sun, 0.8 sun, 0.9 sun, and 1.0 sun, for the anisotropic graphene aerogel and the corresponding PPC, respectively [24].

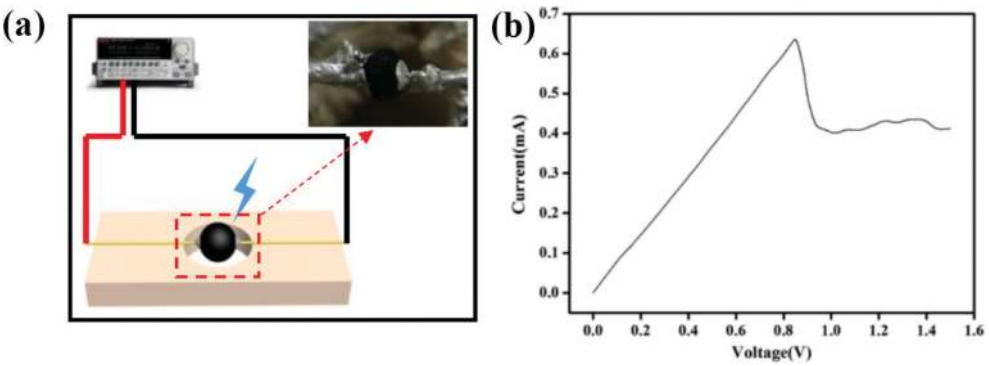

Figure 10. (a) Illustration of the testing process of thermal buffer, (b) current-voltage curve of a single graphene-aerogel-based PCC microsphere [33].

the resistance of the PCC microsphere increased very rapidly, as reflected by the current drop shown in **Figure 10b**. With further increasing the voltage, more PCMs melted, with the current suppressed at the finite value. Clearly, such effect of thermal buffer can effectively protect the circuit upon the overloading of voltage.

5. Conclusion and outlook

We have reviewed recent progresses of graphene-aerogel-based PCCs, in different forms with different dimensions, introduced in detail the sol-gel-based fabrication methods, and demonstrated their potential applications.

Besides these successful achievements, there are still many problems and challenges. For example, it is still easy to cause the reopening of the porous network of graphene under the external strike, leading to the leakage during the service. A higher thermal conductivity is still of strong request for high-performance applications, especially for the directional thermal conductivities. Furthermore, besides the thermal performance, more focus should be paid to the electrical and mechanical properties of PCC. Based on the multifunctionalities of graphene assemblies, smart PCCs are expected to respond to magnetic, heat, moisture, and abrasion. Furthermore, for the stored thermal energy, it is also important to convert it into electrical or mechanical energies by developing PCM-based actuators.

Acknowledgements

This work was financially supported by the National Natural Science Foundation of China (51572285, 21373024), the National Key Research and Development Program of China (2016YFA0203301) and the Natural Science Foundation of Jiangsu Province (BK20170428).

Author details

Guangyong Li[1,2], Xiaohua Zhang[1] and Xuetong Zhang[1]*

*Address all correspondence to: xtzhang2013@sinano.ac.cn

1 Suzhou Institute of Nano-Tech and Nano-Bionics, Chinese Academy of Sciences, Suzhou, P. R. China

2 School of Materials Science and Engineering, Beijing Institute of Technology, Beijing, P. R. China

References

[1] Liu C, Li F, Ma L-P, Cheng H-M. Advanced materials for energy storage. Advanced Materials. 2010;**22**:E28-E62. DOI: 10.1002/adma.200903328

[2] Pielichowska K, Pielichowski K. Phase change materials for thermal energy storage. Progress in Materials Science. 2014;**65**:67-123. DOI: 10.1016/j.pmatsci.2014.03.005

[3] Ji H, Sellan DP, Pettes MT, Kong X, Ji J, Shi L, Ruoff RS. Enhanced thermal conductivity of phase change materials with ultrathin-graphite foams for thermal energy storage. Energy & Environment Science. 2014;**7**:1185-1192. DOI: 10.1039/c3ee42573h

[4] Farid MM, Khudhair AM, Razack SAK, Al-Hallaj S. A review on phase change energy storage: Materials and applications. Energy Conversion and Management. 2004;**45**:1597-1615. DOI: 10.1016/j.enconman.2003.09.015

[5] Wang C., Feng L., Li W., Zheng J., Tian W., Li X.: Shape-stabilized phase change materials based on polyethylene glycol/porous carbon composite: The influence of the pore structure of the carbon materials. Solar Energy Materials & Solar Cells. 2012;**105**:21-26. DOI: 10.1016/j.solmat.2012.05.031

[6] Xiao X, Zhang P, Li M. Preparation and thermal characterization of paraffin/metal foam composite phase change material. Applied Energy. 2013;**112**:1357-1366. DOI: 10.1016/j.apenergy.2013.04.050

[7] Chen L, Zou R, Xia W, Liu Z, Shang Y, Zhu J, Wang Y, Lin J, Xia D, Cao A. Electro- and Photodriven phase change composites based on wax-infiltrated carbon nanotube sponges. ACS Nano. 2012;**6**:10884-10892. DOI: 10.1021/nn304310n

[8] Li Y, Samad YA, Polychronopoulou K, Alhassan SM, Liao K. From biomass to high performance solar-thermal and electric-thermal energy conversion and storage materials. Journal of Materials Chemistry A. 2014;**2**:7759-7765. DOI: 10.1039/c4ta00839a

[9] Liu Z, Zou R, Lin Z, Gui X, Chen R, Lin J, Shang Y, Cao A. Tailoring carbon nanotube density for modulating electro-to-heat conversion in phase change composites. Nano Letter. 2013;**13**:4028-4035. DOI: 10.1021/nl401097d

[10] Liu C, Rao Z, Zhao J, Huo Y, Li Y. Review on nanoencapsulated phase change materials: Preparation, characterization and heat transfer enhancement. Nano Energy. 2015;**13**:814-826. DOI: 10.1016/j.nanoen.2015.02.016

[11] Novoselov KS, Geim AK, Morozov S, Jiang D, Zhang Y, Dubonos S, Grigorieva I, Firsov A. Electric field effect in atomically thin carbon films. Science. 2004;**306**:666-669. DOI: 10.1126/science.1102896

[12] Li C, Shi G. Functional gels based on chemically modified Graphenes. Advanced Materials. 2014;**26**:3992-4012. DOI: 10.1002/adma.201306104

[13] Zeng M, Wang WL, Bai XD. Preparing three-dimensional graphene architectures: Review of recent developments. Chinese Physics B. 2013;**22**: 098105. DOI: 10.1088/1674-1056/22/9/098105

[14] Li Z, Liu Z, Sun H, Gao C. Superstructured assembly of Nanocarbons: Fullerenes, nanotubes, and Graphene. Chemical Reviews. 2015;**115**:7046-7117. DOI: 10.1021/acs.chemrev.5b00102

[15] Chen Z, Ren W, Gao L, Liu B, Pei S, Cheng H-M. Three-dimensional flexible and conductive interconnected graphene networks grown by chemical vapour deposition. Nature Materials. 2011;**10**:424-428. DOI: 10.1038/NMAT3001

[16] Bi H, Lin T, Xu F, Tang Y, Liu Z, Huang F. New Graphene form of Nanoporous monolith for excellent energy storage. Nano Letters. 2015;**16**:349-354. DOI: 10.1021/acs.nanolett.5b03923

[17] Zhang X, Sui Z, Xu B, Yue S, Luo Y, Zhan W, Liu B. Mechanically strong and highly conductive graphene aerogel and its use as electrodes for electrochemical power sources. Journal of Materials Chemistry. 2011;**21**:6494-6497. DOI: 10.1039/c1jm10239g

[18] Xu Y, Sheng K, Li C, Shi G. Self-assembled graphene hydrogel via a one-step hydrothermal process. ACS Nano. 2010;**4**:4324-4330. DOI: 10.1021/nn101187z

[19] Sheng K, Sun Y, Li C, Yuan W, Shi G. Ultrahigh-rate supercapacitors based on eletrochemically reduced graphene oxide for ac line-filtering. Scientific Reports. 2012;**2**: 247. DOI: 10.1038/srep00247

[20] Sui Z, Zhang X, Lei Y, Luo Y. Easy and green synthesis of reduced graphite oxide-based hydrogels. Carbon. 2011;**49**:4314-4321. DOI: 10.1016/j.carbon.2011.06.006

[21] Hu H, Zhao ZB, Wan WB, Gogotsi Y, Qiu JS. Ultralight and highly compressible graphene aerogels. Advanced Materials. 2013;**25**:2219-2223. DOI: 10.1002/adma.201204530

[22] Xu Z, Gao C. Aqueous liquid crystals of graphene oxide. ACS Nano. 2011;**5**:2908-2915. DOI: 10.1021/nn200069w

[23] Kim JE, Han TH, Lee SH, Kim JY, Ahn CW, Yun JM, Kim SO. Graphene oxide liquid crystals. Angewandite Chemite International Edition. 2011;**50**:3043-3047. DOI: 10.1002/anie.201004692

[24] Li G, Zhang X, Wang J, Fang J. From anisotropic graphene aerogels to electron- and photo-driven phase change composites. Journal of Materials Chemistry A. 2016;**4**:17042-17049. DOI: 10.1039/c6ta07587h

[25] Tsotsas E, Mujumdar AS. Modern Drying Technology, Volume 3: Product Quality and Formulation. Chichester: Wiley; 2011. 394 p. DOI: 10.1002/9783527631667

[26] Yang M, Zhao N, Cui Y, Gao W, Zhao Q, Gao C, Bai H, Xie T. Biomimetic architectured graphene aerogel with exceptional strength and resilience. ACS Nano. 2017;**11**:6817-6824. DOI: 10.1021/acsnano.7b01815

[27] Zhang P, Li J, Lv L, Zhao Y, Qu L. Vertically aligned graphene sheets membrane for highly efficient solar thermal generation of clean water. ACS Nano. 2017;**11**:5087-5093. DOI: 10.1021/acsnano.7b01965

[28] Zhao X, Yao W, Gao W, Chen H, Gao C. Wet-spun superelastic graphene aerogel millispheres with group effect. Advanced Materials. 2017;**29**. DOI: 10.1002/adma.201701482

[29] Zhang L, Li R, Tang B, Wang P. Solar-thermal conversion and thermal energy storage of graphene foam-based composites. Nanoscale. 2016;**8**:14600-14607. DOI: 10.1039/c6nr03921a

[30] Cai H, Sharma S, Liu W, Mu W, Liu W, Zhang X, Deng Y. Aerogel microspheres from natural cellulose nanofibrils and their application as cell culture scaffold. Biomacromolecules. 2014;**15**:2540-2547. DOI: 10.1021/bm5003976

[31] Zhang C, Zhai T, Turng L-S. Aerogel microspheres based on cellulose nanofibrils as potential cell culture scaffolds. Cellulose. 2017;**24**:2791-2799. DOI: 10.1007/s10570-017-1295-9

[32] Park SH, Kim HK, Yoon SB, Lee CW, Ahn D, Lee SI, Roh KC, Kim KB. Spray-assisted deep-frying process for the in situ spherical assembly of graphene for energy-storage devices. Chemistry of Materials. 2015;**27**:457-465. DOI: 10.1021/cm5034244

[33] Wang X, Li G, Hong G, Guo Q, Zhang X. Graphene aerogel templated fabrication of phase change microspheres as thermal buffers in microelectronic devices. ACS Applied Materials & Interfaces. 2017;**9**:41323-41331. DOI: 10.1021/acsami.7b13969

[34] Mondal S. Phase change materials for smart textiles - an overview. Applied Thermal Engineering. 2008;**28**:1536-1550. DOI: 10.1016/j.applthermaleng.2007.08.009

[35] Jesse TMC, Manuel M, Xia Y. Melt coaxial electrospinning: A versatile method for the encapsulation of solid materials and fabrication of phase change nanofibers. Nano Letters. 2006;**6**:2868-2872. DOI: 10.1021/nl0620839

[36] Chen C, Wang L, Huang Y. Electrospun phase change fibers based on polyethylene glycol/cellulose acetate blends. Applied Energy. 2011;**88**:3133-3139. DOI: 10.1016/j.apenergy.2011.02.026

[37] Wen GQ, Xie R, Liang WG, He XH, Wang W, Ju XJ, Chu LY. Microfluidic fabrication and thermal characteristics of core–shell phase change microfibers with high paraffin content. Applied Thermal Engineering. 2015;**87**:471-480. DOI: 10.1016/j.applthermaleng.2015.05.036

[38] Xu Z, Zhang Y, Li PG, Gao C. Strong: Conductive, lightweight, neat graphene aerogel fibers with aligned pores. ACS Nano. 2012;**6**:7103-7113. DOI: 10.1021/nn3021772

[39] Yu D, Goh K, Wang H, Wei L, Jiang W, Zhang Q, Dai L, Chen Y. Scalable synthesis of hierarchically structured carbon nanotube-graphene fibres for capacitive energy storage. Nature Nanotechnology. 2014;**9**:555. DOI: 10.1038/NNANO.2014.93

[40] Liu Z, Li Z, Xu Z, Xia Z, Hu X, Kou L, Peng L, Wei Y, Gao C. Wet-spun continuous graphene films. Chemistry of Materials. 2014;**26**:6786-6795. DOI: 10.1021/cm5033089

[41] Kou L, Liu Z, Huang T, Zheng B, Tian Z, Deng Z, Gao C. Wet-spun, porous, orientational graphene hydrogel films for high-performance supercapacitor electrodes. Nanoscale. 2015;**7**:4080-4087. DOI: 10.1039/c4nr07038k

[42] Xiong Z, Liao C, Han W, Wang X. Mechanically tough large-area hierarchical porous Graphene films for high-performance flexible Supercapacitor applications. Advanced Materials. 2015;**27**:4469-4475. DOI: 10.1002/adma.201501983

[43] Ye S, Zhang Q, Hu D, Feng J. Core-shell-like structured graphene aerogel encapsulating paraffin: Shape-stable phase change material for thermal energy storage. Journal of Materials Chemistry A. 2015;**3**:4018-4025. DOI: 10.1039/c4ta05448b

[44] Zhong Y, Zhou M, Huang F, Lin T, Wan D. Effect of graphene aerogel on thermal behavior of phase change materials for thermal management. Solar Energy Materials & Solar Cells. 2013;**113**:195-200. DOI: 10.1016/j.solmat.2013.01.046

[45] Zhang K, Han B, Xun Y. Electrically conductive carbon nanofiber/paraffin wax composites for electric thermal storage. Energy Conversion & Management. 2012;**64**:62-67. DOI: 10.1016/j.enconman.2012.06.021